

Fibroblast fate determination during cardiac reprogramming by remodeling of actin filaments

Zhentao Zhang,^{1,2,3} Wenhui Zhang,^{1,2,3} Robert Blakes,^{1,2,3} Lauren J. Sundby,⁵ Zengdun Shi,⁶ Don C. Rockey,⁶ James M. Ervasti,^{4,5} and Young-Jae Nam^{1,2,3,*}

¹Department of Medicine, Division of Cardiovascular Medicine, Vanderbilt University Medical Center, Nashville, TN, USA

²Department of Cell and Developmental Biology, Vanderbilt University, Nashville, TN, USA

³Vanderbilt Center for Stem Cell Biology, Vanderbilt University, Nashville, TN, USA

⁴Department of Biochemistry, Molecular Biology and Biophysics, University of Minnesota, Minneapolis, MN, USA

⁵Program in Molecular, Cellular, Developmental Biology, and Genetics, University of Minnesota, Minneapolis, MN, USA

⁶Department of Internal Medicine, Medical University of South Carolina, Charleston, SC, USA

*Correspondence: young-jae.nam@vumc.org

<https://doi.org/10.1016/j.stemcr.2022.05.004>

SUMMARY

Fibroblasts can be reprogrammed into induced cardiomyocyte-like cells (iCMs) by forced expression of cardiogenic transcription factors. However, it remains unknown how fibroblasts adopt a cardiomyocyte (CM) fate during their spontaneous ongoing transdifferentiation toward myofibroblasts (MFs). By tracing fibroblast lineages following cardiac reprogramming *in vitro*, we found that most mature iCMs are derived directly from fibroblasts without transition through the MF state. This direct conversion is attributable to mutually exclusive induction of cardiac sarcomeres and MF cytoskeletal structures in the cytoplasm of fibroblasts during reprogramming. For direct fate switch from fibroblasts to iCMs, significant remodeling of actin isoforms occurs in fibroblasts, including induction of α -cardiac actin and decrease of the actin isoforms predominant in MFs. Accordingly, genetic or pharmacological ablation of MF-enriched actin isoforms significantly enhances cardiac reprogramming. Our results demonstrate that remodeling of actin isoforms is required for fibroblast to CM fate conversion by cardiac reprogramming.

INTRODUCTION

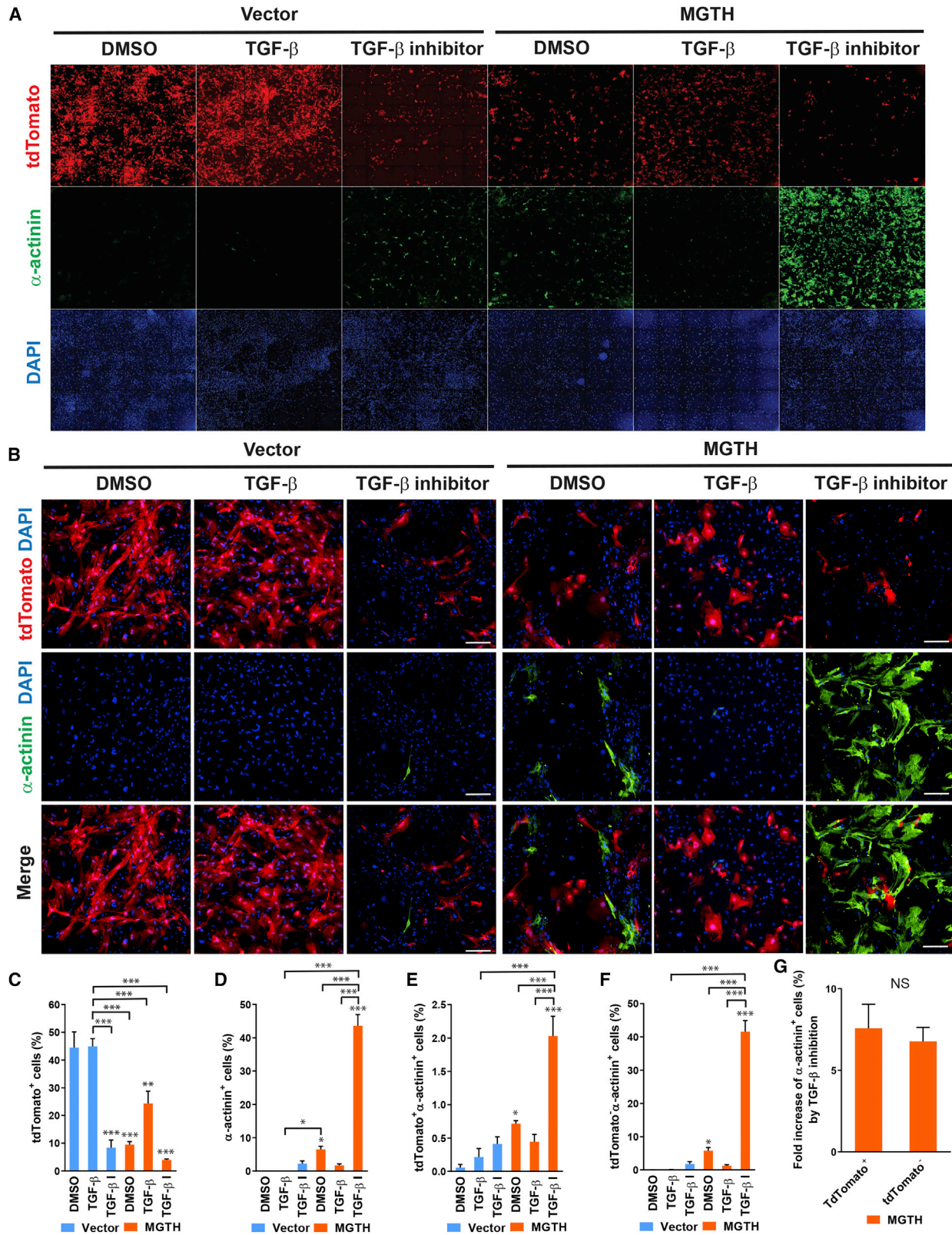
Ischemic heart disease leading to myocardial infarction (MI) is a primary cause of morbidity and mortality worldwide (Benjamin et al., 2018). Owing to little regenerative capacity of the heart, the massive loss of cardiomyocytes (CMs) after MI is replaced by cardiac fibrosis. Although cardiac fibrosis is initially essential for maintaining cardiac structure and preventing cardiac rupture, progressive cardiac fibrosis can destroy the mechanical architecture of the myocardium and thus contribute to cardiac dysfunction and adverse remodeling, thereby leading to heart failure. Thus, the approach of reprogramming cardiac fibroblasts to induced cardiomyocyte-like cells (iCMs) is particularly attractive in that it directly targets cardiac fibroblasts, the main culprits of fibrosis, to redirect their fates and induce new CMs. This concept was first demonstrated *in vitro* using three cardiogenic transcription factors, namely Gata4, Mef2c, and Tbx5 (Ieda et al., 2010). Addition of another transcription factor, Hand2, has been shown to improve cardiac reprogramming (Song et al., 2012; Umei et al., 2017; Zhang et al., 2019a, 2019b). Alternatively, combination of microRNAs and chemicals has also been shown to reprogram fibroblasts to iCMs (Fu et al., 2015; Jayawardena et al., 2012). Importantly, it was also demonstrated that the reprogramming approach can convert resident cardiac fibroblasts to iCMs in the heart after heart injury (Inagawa et al., 2012; Qian et al., 2012;

Song et al., 2012), suggesting its therapeutic potential as a post-MI intervention.

Although the cardiac reprogramming approach potentially offers a promising source of new CMs, this strategy still remains a proof-of-concept approach, at least in part, owing to our limited understanding of reprogramming processes. For example, it is unknown how and when a fibroblast, which is in the process of its own phenotypic changes, adopts a new CM fate during cardiac reprogramming. Following injury, loss of CMs triggers the recruitment of a variety of inflammatory cells to the injured area to remove necrotic CMs (Humeres and Frangogiannis, 2019). Meanwhile, cardiac fibroblasts are activated, proliferated, and transdifferentiated into myofibroblasts (MFs), thereby populating the infarcted area. MFs secrete extracellular matrix proteins to form scar tissue. The heart seals off the CM-deficient, injured area with collagen-based scar tissue. This is how the heart with little regenerative capacity repairs itself after injury. However, it remains elusive how the reprogramming process can negotiate the necessary and dynamic default fibrogenic repair process to induce new CMs.

In this study, we sought to determine how a fibroblast changes its cell fate to become an iCM in the context of its dynamic ongoing differentiation processes by tracing fibroblast fate paths. We found that most fibroblasts do not go through the MF fate path to become mature iCMs. We further demonstrated that remodeling of actin isoforms





(legend on next page)



is necessary for a fibroblast to fully commit to a myogenic fate during cardiac reprogramming by developing sarcomeres as well as by repressing organization of MF actin filaments in the fibroblast cytoplasm. Our study suggests that the structural conflict between MF cytoskeleton and sarcomere formation determines fibroblast fate during cardiac reprogramming.

RESULTS

Most structurally and functionally defined iCMs are derived directly from fibroblasts without transition through the MF state

A simple way to induce fibroblast to MF differentiation is to culture fibroblasts on a conventional plastic culture dish (van Putten et al., 2016). Because of isometric tension created by a plastic dish's stiffness, fibroblasts spontaneously differentiate to MFs. This *in vitro* process resembles MF differentiation due to extracellular matrix stiffening in the setting of fibrotic injury *in vivo*. We used this simple cell-based system along with transforming growth factor β (TGF- β) stimulation and inhibition to demonstrate fibroblast fate paths during cardiac reprogramming. TGF- β signaling is a potent inducer of MF activation (Leask, 2007). It has been well documented that inhibition of TGF- β signaling enhances cardiac reprogramming, while its overactivation inhibits it (Ifkovits et al., 2014; Kurotsu et al., 2020; Mohamed et al., 2016; Zhao et al., 2015). To trace MF lineages during cardiac reprogramming, we used mouse embryonic fibroblasts (MEFs) isolated from α SMA^{Cre}:R26R^{tdT} mice generated by crossing α SMA^{Cre} mice (LeBleu et al., 2013) with Rosa26-CAG-LoxP-stop-LoxP-tdTomato (tdT) mice, since neoexpression of α -smooth muscle actin (α SMA) is a hallmark of MFs (Darby et al., 1990). tdT is permanently expressed in a cell carrying both α SMA^{Cre} and R26R^{tdT} alleles by Cre-mediated excision of stop cassette upon activation of α SMA promoter. In other words, when fibroblasts differentiate to myofibroblasts, tdT is irreversibly turned on in α SMA⁺ MFs in this system, thereby allowing us to trace the cells derived from α SMA⁺ MFs. We transduced MEFs isolated from α SMA^{Cre}:R26R^{tdT} mice with MGTH or vector and exposed

the transduced cells to dimethyl sulfoxide (DMSO), TGF- β , or TGF- β inhibitors. We analyzed expression of tdT and α -actinin using high-content imaging analysis after 4 weeks (Figure 1). tdT⁺ cells indicate α SMA⁺ MF lineage traced cells, while α -actinin⁺ cells represent cells reprogrammed toward a CM fate. Accordingly, tdT⁺ α -actinin⁺ or tdT⁻ α -actinin⁺ cells may represent the reprogrammed cells with or without transitioning through an α SMA⁺ MF state, respectively. We found that ~45% of vector transduced cells treated with DMSO or TGF- β express tdT, indicating that these cells are differentiated to MFs (Figure 1C). There was no significant difference in tdT expression between DMSO and TGF- β exposed vector transduced cells, probably because isometric tension provided by a stiff plastic culture plate was sufficient to induce MF activation without TGF- β stimulation. In contrast, TGF- β inhibition significantly repressed tdT expression in vector transduced cells (~8%). Importantly, MGTH transduction significantly reduced tdT⁺ cells (%) with DMSO (~10%), and further reduced it along with TGF- β inhibitors (~4%). These results indicated that MGTH transduction alone significantly inhibits MF transformation. It may explain the limited additional repressive effect of TGF- β inhibitor on MF activation in the context of MGTH transduction. MGTH transduction with TGF- β inhibitor treatment markedly increased α -actinin⁺ cells (%), as opposed to DMSO- or TGF- β -treated cells (Figure 1D). While decrease of tdT expression was not markedly different between TGF- β inhibitor and DMSO-treated MGTH transduced cells (~4% versus ~10%), increase of α -actinin induction by TGF- β inhibition was far greater than DMSO treatment (~44% versus ~7%). These results suggest that enhancement of cardiac reprogramming by TGF- β inhibition is not mainly due to repression of MF activation in the context of MGTH transduction. At most ~2% of cells following MGTH transduction with TGF- β inhibition were tdT⁺ α -actinin⁺, indicating that these cells are derived from α SMA⁺ MFs. In contrast, most α -actinin⁺ cells did not express tdT, indicating that these cells are derived directly from α SMA⁻ fibroblasts (Figures 1E and 1F). Although the number of α -actinin⁺tdT⁺ cells is very small, the fold increase in the percentage of α -actinin⁺ cells among tdT⁺ cells

Figure 1. Fibroblast fate paths toward iCMs during cardiac reprogramming

- (A) Representative composite immunofluorescent images used for high-content imaging analyses to quantify tdT⁺ and α -actinin⁺ cells. Each panel shows a composition of 36 images taken by the high-content imaging system.
- (B) Representative individual immunofluorescent images used for high-content imaging analyses following indicated transductions and treatments. Scale bars, 200 μ m.
- (C–F) Summary of quantification of tdT⁺ and/or α -actinin⁺ cells. Six independent experiments are presented as mean \pm SD. * p < 0.05, ** p < 0.005, or *** p < 0.0001 versus vector transduction with DMSO treatment. Other comparisons are statistically non-significant unless otherwise indicated. TGF- β I, TGF- β inhibitors.
- (G) Comparison of the effect of TGF- β inhibition on increased induction of α -actinin⁺ cells between tdT⁺ and tdT⁻ cells. Six independent experiments are presented as mean \pm SD. NS, not significant (p > 0.05).



(α -actinin⁺tdT⁺/tdT⁺) by TGF- β inhibition over DMSO treatment is similar to the counterpart of tdT⁻ cells (α -actinin⁺tdT⁻/tdT⁻) in the context of MGTH transduction (Figure 1G). These results also suggest the positive effect of TGF- β inhibition on cardiac reprogramming independent of its repression of MF activation. We speculate that substantial inhibition of MF activation by MGTH transduction may limit additive effects of TGF- β inhibition on enhanced cardiac reprogramming by suppressing myofibroblast activation when both are applied to fibroblasts. Next, we sought to determine the quality of tdT⁺ reprogrammed cells by examining their sarcomeric structures. We quantified the percentage of cells exhibiting well-organized sarcomeres labeled by both α -actinin and Myomesin among tdT⁺ and tdT⁻ cells. While ~2% of tdT⁻ cells demonstrated well-organized sarcomeres, tdT⁺ cells rarely developed sarcomeres (Figures 2A and 2B). In addition, most beating iCMs were tdT⁻ (Figures 2C and 2D; Video S1). Taken together, our results showed that most structurally and functionally defined iCMs are not derived from α SMA⁺ MF lineage traced cells.

Unexpectedly, we observed induction of α -actinin⁺ cells with TGF- β inhibition along with vector transduction (Figure 1). To determine whether TGF- β inhibition alone is sufficient to reprogram fibroblasts to iCMs, we examined sarcomere formation by TGF- β inhibition alone. We did not observe well-organized sarcomeres in TGF- β inhibitor treated cells without MGTH transduction, while we observed a significant number of cells exhibiting sarcomere assembly in MGTH transduced cells with or without TGF- β inhibition (Figures S1A and S1B). In addition, we did not observe beating cells without MGTH transduction (data not shown). We also analyzed the cardiac and fibroblast gene profile following vector or MGTH transduction with or without TGF- β inhibitor exposure using qPCR. Vector transduction with TGF- β inhibition showed a noticeable trend toward increased expression of cardiac genes as well as decreased expression of fibroblast genes compared with vector transduction with DMSO treatment (Figure S1C). However, the degree of cardiac gene activation and fibroblast gene repression by TGF- β inhibition alone was much lower than MGTH transduction with or without TGF- β inhibition. Taken together, our results indicate that although TGF- β inhibition alone may affect cardiac and fibroblast gene programs, it was far from sufficient to induce iCMs that are structurally organized and functionally active.

α SMA incorporation into stress fibers inhibits structural and functional progression of iCMs

An important next question was how either an MF or iCM fate of fibroblasts is determined during cardiac reprogramming. Fibroblasts develop their own contractile structures in response to isometric mechanical tension created by a

stiff plastic culture plate *in vitro* or fibrotic processes during tissue injury *in vivo* (Sandbo and Dulin, 2011; Tomasek et al., 2002). This mechanical stimulus activates downstream signaling pathways for MF transformation (Tschumperlin et al., 2018). As a result, fibroblasts induce stress fibers, actin-myosin bundles crosslinked by non-muscle α -actinin, for generating isometric contractile force (Hotulainen and Lappalainen, 2006) (Figure 3A, top). To augment isometric tension, α SMA is induced and incorporated into stress fibers (Hinz et al., 2001) (Figure 3A, middle). Such cells that contain α SMA incorporated stress fibers are commonly defined as an MF (Hinz, 2010; Sandbo and Dulin, 2011). CMs and iCMs also contain similar actin-myosin-based contractile structures, which are known as sarcomeres (Figure 3A, bottom). Although CMs and iCMs also have actin-myosin-based structures, they are structurally distinct from MFs. First, the sarcomeres in iCMs (and CMs) are precisely aligned (Gautel, 2011), in contrast to its counterpart in MFs (Hotulainen and Lappalainen, 2006) (Figure 3A, white inlet). Second, Titin is a critical component in the sarcomere of striated muscle while it is absent in stress fibers. Titin connects thin filament (actin-based structure) with thick filament (myosin-based structure), thereby organizing the regular interdigitation of the thick and thin filaments in the myofibrillar lattice and allowing isotonic mechanical shortening of the sarcomere (Clark et al., 2002). Third, the molecular composition of stress fiber is similar but not identical to the sarcomere. For example, β -actin and γ -actin are major actin components of stress fibers in fibroblasts (Sandbo and Dulin, 2011), while α -cardiac actin is a major actin isoform in the cardiac sarcomere (Perrin and Ervasti, 2010). These distinct actin-myosin-based contractile structures (i.e., stress fiber and sarcomere) are simultaneously developed in fibroblasts during cardiac reprogramming. Thus, we hypothesized that development of distinct and mutually exclusive contractile structures in fibroblasts determines fibroblast fate during cardiac reprogramming. It seems intuitive that sarcomere assembly would be unsuccessful when stress fibers are already well organized in the fibroblast cytoplasm, and vice versa. We examined simultaneous development of α SMA incorporated stress fibers and cardiac sarcomeres following reprogramming MEFs isolated from Titin-eGFP knockin reporter mice. Sarcomeres represented by M-bands are unequivocally marked by eGFP in this mouse line in which eGFP was inserted into M-band exon 6 of *titin* (da Silva Lopes et al., 2011). Since Titin filaments, which serve as a blueprint of sarcomere assembly (Clark et al., 2002), are completely absent in stress fibers, demonstrating their presence is a reliable approach to differentiate sarcomere assembly from stress fiber formation during cardiac reprogramming. Four weeks after MGTH transduction, we immunolabeled cells to detect GFP and α SMA. We found that reprogrammed cells exhibiting

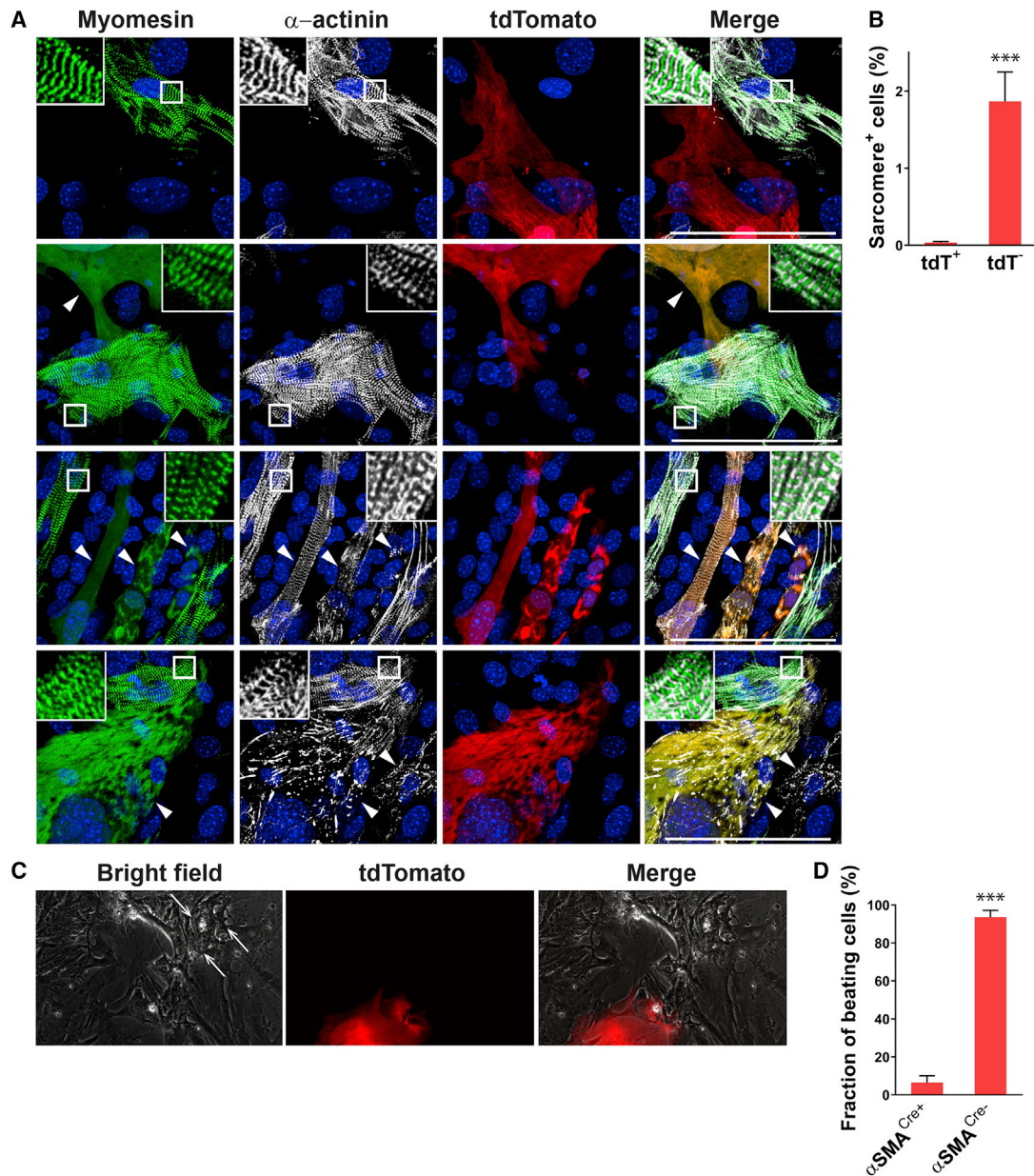


Figure 2. Assessment of sarcomere assembly and contractility in tdT⁺ and tdT⁻ cells following MGTH transduction into α SMA^{Cre}:R26R^{tdT} MEFs

MEFs isolated from α SMA^{Cre}:R26R^{tdT} mice were transduced with MGTH and exposed to TGF- β inhibitors.

(A) Cells were immunostained for Myomesin and α -actinin 4 weeks post transduction. Sarcomere assembly was defined by M-band structures detected by Myomesin expression and Z-disc structures detected by α -actinin expression. Enlarged views in insets show M-band structures and Z-disc structures in sarcomeres. Arrowheads indicate the cells that express α -actinin and/or Myomesin but fail to fully assemble sarcomeres. Scale bars, 100 μ m.

(B) The percentage of cells exhibiting both M-bands and Z-discs was quantified. Six independent experiments are presented as mean \pm SD. ***p < 0.001.

(C) Live bright-field and red fluorescent images and videos were captured 4 weeks post transduction. Arrows indicate the beating iCMs in Video S1. Scale bar, 100 μ m.

(D) The percentage of α SMA^{Cre+} or α SMA^{Cre-} cells among beating iCMs was quantified. Six independent experiments are presented as mean \pm SD. ***p < 0.0001.

See also Video S1.

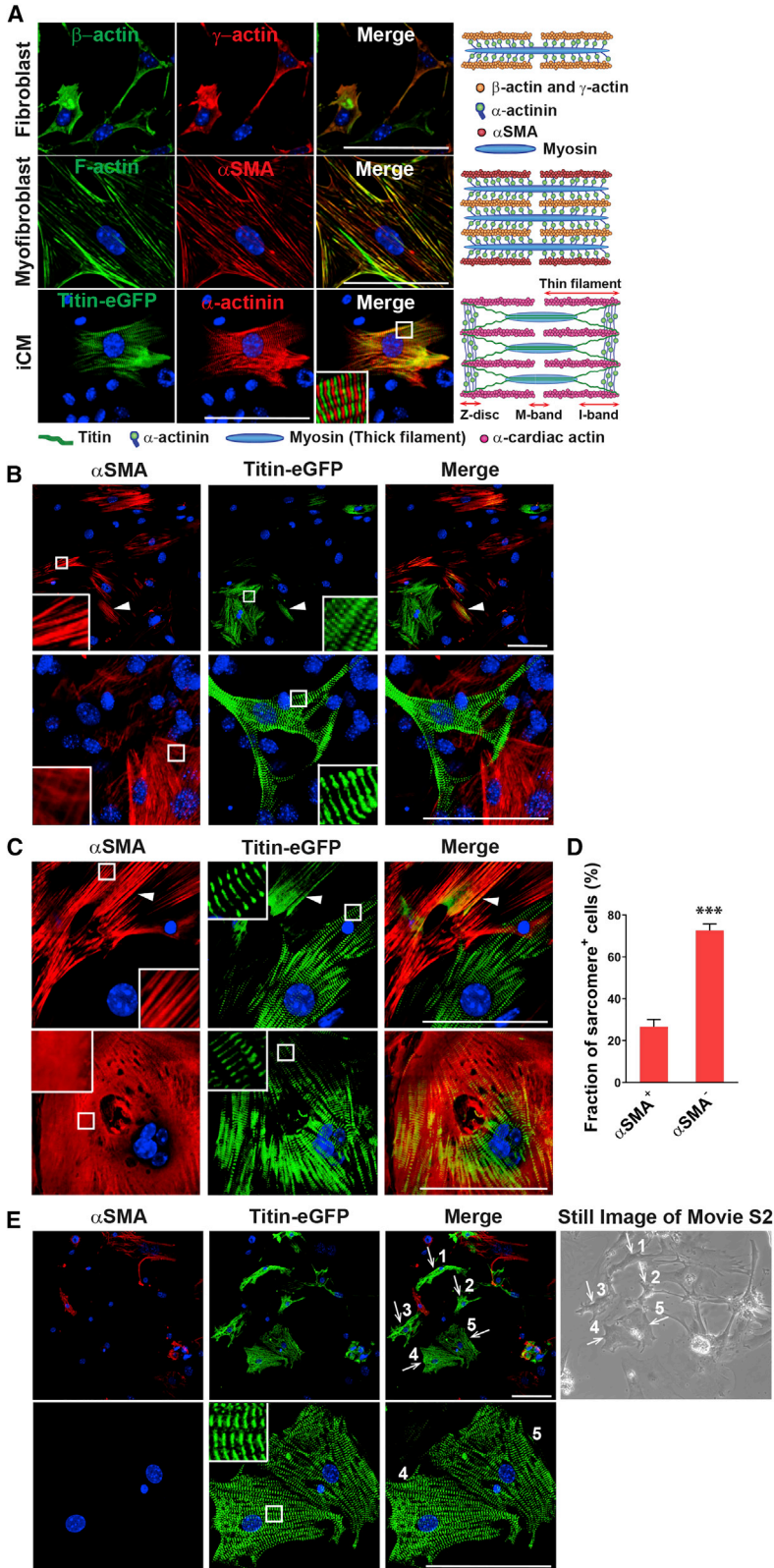


Figure 3. Sarcomeres are not co-induced with α SMA⁺ stress fibers during cardiac reprogramming

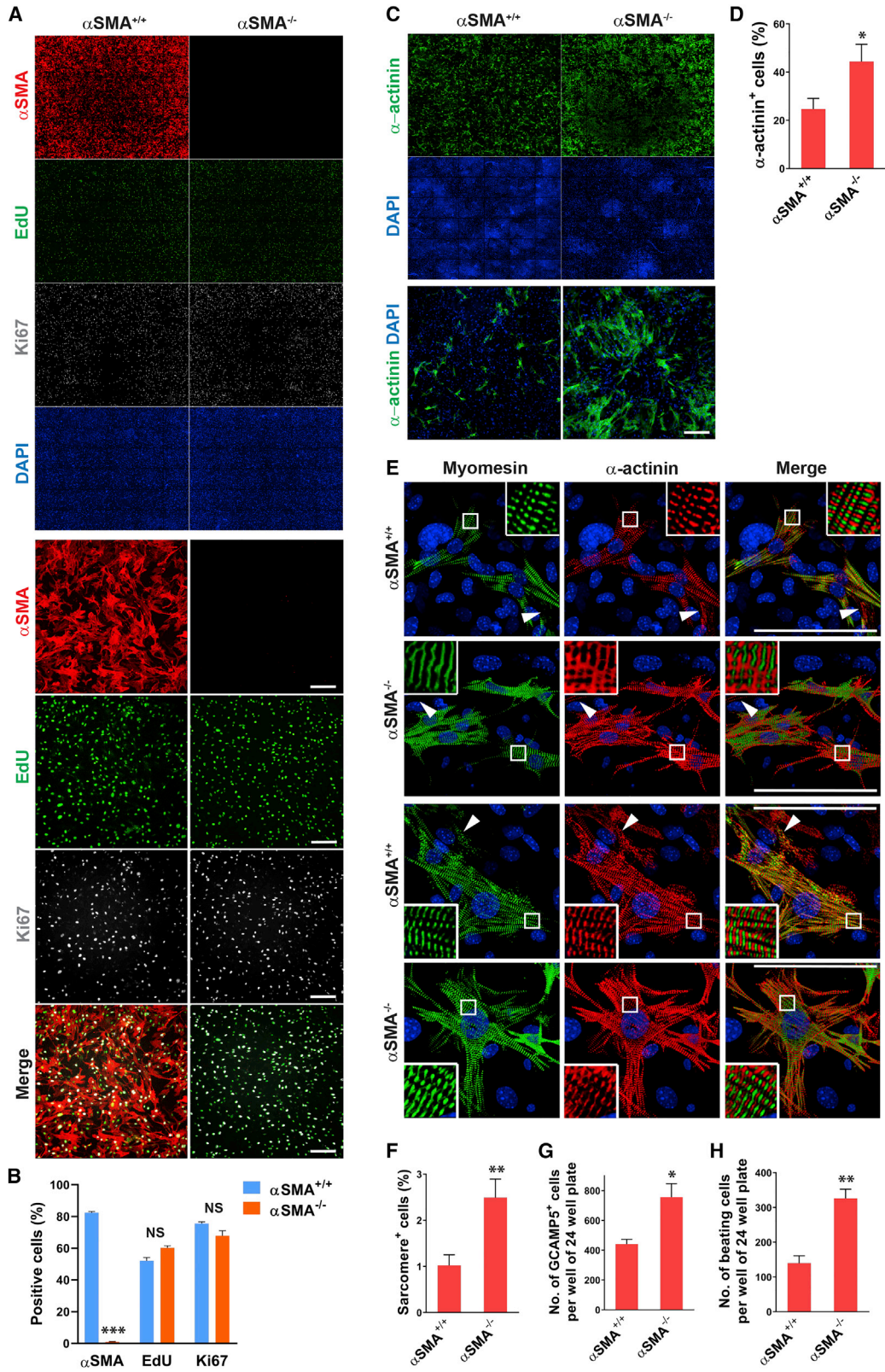
(A) Demonstration of cytoskeletal structures of fibroblasts, MFs, and iCMs by immunostaining, and a schematic illustration. MEFs were immunostained for β -actin and γ -actin 1 day after plating on a plastic culture dish (top). MFs were immunostained for α SMA and stained for F-actin with phalloidin 1 week after plating MEFs on a plastic culture dish (middle). At 4 weeks after transduction of MGTH into Titin-eGFP MEFs, iCMs were immunostained for Titin-eGFP and α -actinin (bottom). Enlarged views in insets show M-band (Titin-eGFP) and Z-disc (α -actinin) structures in sarcomeres. Scale bars, 100 μ m.

(B and C) Mutually exclusive development of stress fibers and sarcomeres in fibroblasts during cardiac reprogramming. Enlarged views in insets show M-band structures in sarcomeres or α SMA⁺ stress fibers. Scale bars, 100 μ m.

(D) Inverse relationship between sarcomere formation and α SMA expression during cardiac reprogramming. The percentage of α SMA⁺ or α SMA⁻ cells among cells exhibiting organized sarcomeres was quantified. Twelve independent experiments are presented as mean \pm SD. *** $p < 0.0001$.

(E) Absence of α SMA⁺ stress fiber in contractile iCMs. Beating iCMs were identified 4 weeks after MGTH transduction into Titin-eGFP MEFs. After videos of beating iCMs were recorded, cells were immunostained for Titin-eGFP and α SMA. The beating iCMs were correlated with immunostained cells. Enlarged views in insets show M-band structures in sarcomeres. Arrows in the immunofluorescent image indicate the beating iCMs with the corresponding numbers in the still image of [Video S2](#). Scale bars, 100 μ m.

See also [Video S2](#).



(legend on next page)



M-band structures did not show α SMA⁺ stress fibers (Figure 3B). However, we identified Titin-eGFP⁺ cells without establishing M-band structures in the context of α SMA expression or stress fiber formation (arrowheads in Figures 3B and 3C) and α SMA⁺ cells without establishing organized stress fibers in the context of sarcomere formation (Figure 3C, bottom). A majority of iCMs exhibiting well-organized sarcomeres did not express α SMA (Figure 3D). To determine the relationship between development of α SMA⁺ stress fibers and functionality of iCMs, we identified beating iCMs and then retrospectively immunostained them for GFP and α SMA. All beating iCMs exhibited highly organized sarcomeres while they lacked α SMA⁺ stress fibers (Figure 3E and Video S2). Taken together, these results suggest that organization of MF actin cytoskeleton by incorporating α SMA into fibroblast actin filaments counteracts induction of myofibrillar structures, which have to be built on the same fibroblast cytoplasm.

The results showing mutually exclusive developments of sarcomeres and α SMA incorporated stress fibers suggest that sarcomere formation competes with structural development of MFs in the cytoplasm of fibroblasts. Thus, we hypothesized that repressing α SMA incorporation into the fibroblast cytoskeleton enhances cardiac reprogramming by tipping the balance toward sarcomere development in the cytoplasm of fibroblasts. To test this hypothesis, we isolated MEFs from α SMA knockout (α SMA^{-/-}) or their wild-type (WT) littermate (α SMA^{+/+}) embryos (Schildmeyer et al., 2000) and demonstrated nearly absent α SMA expression in α SMA^{-/-} MEFs (Figures 4A and 4B). Given that the fibroblast proliferation status can affect cardiac reprogramming (Bektik et al., 2018), we assessed proliferation of α SMA^{+/+} and α SMA^{-/-} MEFs using 5-ethynyl-2'-deoxyuridine (EdU) labeling and Ki67 immunostaining. We found that there was no significant difference in cell proliferation between α SMA^{+/+} and α SMA^{-/-} MEFs (Figures 4A and 4B).

Four weeks after MGTH transduction into α SMA^{+/+} or α SMA^{-/-} MEFs, we immunolabeled cells to detect sarcomeric α -actinin and quantified α -actinin⁺ cells (%) (Figures 4C and 4D). α SMA^{-/-} MEFs more efficiently induce α -actinin than α SMA^{+/+} MEFs. To demonstrate sarcomeric Z-disc and M-band structures in reprogrammed cells, we immunostained them for α -actinin and Myomesin (Figure 4E) and quantified the percentage of cells clearly exhibiting both Z-discs and M-bands using high-magnification images captured by a high-content imaging system. More sarcomere⁺ cells defined by development of both Z-disc and M-band structures were found in α SMA^{-/-} MEFs than in α SMA^{+/+} MEFs (Figure 4F). These results indicate that deletion of α SMA facilitates sarcomere assembly during cardiac reprogramming, probably by suppressing the organization of stress fibers with α SMA incorporation. Next, we assessed calcium handling of reprogrammed cells derived from α SMA^{+/+} and α SMA^{-/-} MEFs using genetically encoded GFP-based calcium indicator (GCaMP). Four weeks after sequentially transducing TroponinT-GCaMP5-Zeo reporter construct (Addis et al., 2013) and MGTH into α SMA^{+/+} and α SMA^{-/-} MEFs, we quantified the number of cells exhibiting spontaneous oscillation of real-time GCaMP5 fluorescence (Figure 4G; Videos S3 and S4). We observed more GCaMP⁺ cells in α SMA^{-/-} MEFs than in α SMA^{+/+} MEFs. As expected, there were significantly more beating cells in α SMA^{-/-} MEF cultures than in controls following MGTH transduction (Figure 4H; Videos S5 and S6). We also analyzed the expression of cardiac and fibroblast genes following MGTH transduction into α SMA^{+/+} and α SMA^{-/-} MEFs using qPCR. Expression of cardiac genes was significantly increased, whereas expression of fibroblast genes was not significantly changed in α SMA^{-/-} MEFs compared with α SMA^{+/+} MEFs (Figure S2). These results suggest that α SMA depletion can further influence cardiac gene programs without significantly affecting fibroblast genes,

Figure 4. Genetic deletion of α SMA enhances cardiac reprogramming

(A and B) α SMA expression and proliferation status in α SMA^{+/+} and α SMA^{-/-} MEFs. α SMA⁺, EdU⁺, or Ki67⁺ cells were quantified using high-content imaging analysis. Representative composite images used for high-content imaging analysis (top) and individual 10 \times images (bottom) are presented (A). Scale bars, 200 μ m. Quantification of α SMA⁺, EdU⁺, or Ki67⁺ cells is summarized (B). Three independent experiments are presented as mean \pm SD. ***p < 0.0001; NS, not significant (p > 0.05).

(C and D) Increase of sarcomeric protein induction by loss of α SMA. α -actinin⁺ cells were quantified using high-content imaging analysis. Representative composite images used for high-content imaging analysis (top) and individual 10 \times images (bottom) are shown (C). Quantification of α -actinin⁺ cells is summarized (D). Twelve independent experiments are presented as mean \pm SD. *p < 0.05.

(E and F) Enhanced sarcomere formation by loss of α SMA. Sarcomere assembly of reprogrammed cells was visualized using a confocal microscope (E). Scale bars, 100 μ m. Enlarged views in insets show M-band structures (Myomesin) and/or Z-disc structures (α -actinin) in sarcomeres. Arrowheads indicate the cells that express α -actinin and/or Myomesin but fail to assemble sarcomeres. The percentage of cells exhibiting organized sarcomeres among the whole population of cells is quantified (F). Six independent experiments are presented as mean \pm SD. **p < 0.01.

(G) Quantification of GCaMP⁺ cells following MGTH transduction into α SMA^{+/+} or α SMA^{-/-} MEFs. Calcium oscillation identified by flashing green fluorescence was quantified. Four independent experiments are presented as mean \pm SD. *p < 0.05. See also Videos S3 and S4.

(H) Quantification of beating iCMs following MGTH transduction into α SMA^{+/+} or α SMA^{-/-} MEFs. Four independent experiments are presented as mean \pm SD. **p < 0.01. See also Videos S5 and S6.

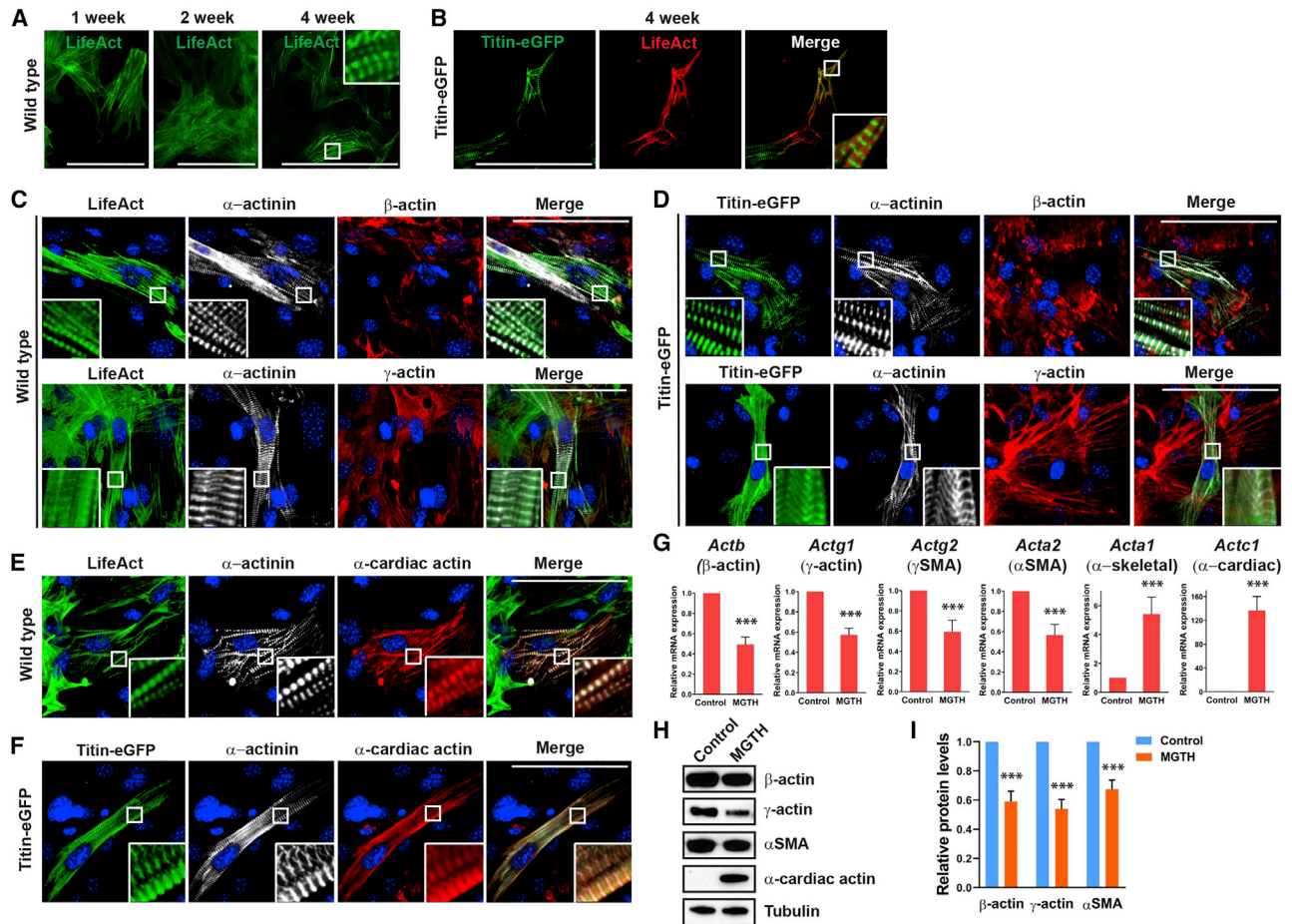


Figure 5. Remodeling of actin isoforms during cardiac reprogramming

(A and B) LifeAct expression during cardiac reprogramming. A retroviral LifeAct-mEmerald (A) or LifeAct-tdT (B) construct was co-transduced with MGTH into WT or Titin-eGFP MEFs, respectively. Videos were recorded to demonstrate beating iCMs 4 weeks post transduction. An enlarged view in an inset shows actin filaments in sarcomeres. Scale bars, 100 μ m. See also [Videos S7](#) and [S8](#).

(C and D) Absence of β -actin and γ -actin expression in iCMs exhibiting sarcomere assembly. Enlarged views in insets show Z-disc (α -actinin) and actin filament (LifeAct) (C) or M-band (Titin-eGFP) (D) in sarcomeres. Scale bars, 100 μ m.

(E and F) Induction of α -cardiac actin during cardiac reprogramming. Enlarged views in insets show Z-discs and actin filaments (LifeAct and α -cardiac actin) (E) and Z-discs, actin filaments (α -cardiac actin), and M-bands (F) in sarcomeres. Scale bars, 100 μ m.

(G) mRNA expression levels of six actin isoforms following cardiac reprogramming using qPCR. Six independent experiments are presented as mean \pm SD. *** p < 0.0001.

(H) Protein expression levels of actin isoforms following cardiac reprogramming using immunoblotting.

(I) Quantification of the intensity of immunoblot bands by densitometry. Three independent experiments are presented as mean \pm SD. *** p < 0.0001.

which are severely repressed by MGTH ([Figure S1C](#)). Taken together, our results indicate that repressing α SMA expression in fibroblasts or α SMA incorporation into the fibroblast cytoskeleton enhances induction of myofibrillar structures in fibroblasts by cardiac reprogramming.

Remodeling of actin isoforms during cardiac reprogramming

To further investigate the role of actins during cardiac reprogramming, we generated a retroviral vector encoding

LifeAct, which is a short actin-binding peptide fused with a fluorescent reporter for visualization of filamentous actin structures ([Riedl et al., 2008](#)). We co-transduced MGTH and a LifeAct-mEmerald or -tdT retroviral vector into WT or Titin-eGFP MEFs, respectively. While stress fiber filaments were visualized by LifeAct at days 7 and 14 post transduction, well-organized sarcomeres labeled with LifeAct were identified in beating iCMs 4 weeks after transduction ([Figures 5A](#) and [5B](#); [Videos S7](#) and [S8](#)). All actin isoforms (i.e., β -actin, γ -actin, α SMA, γ SMA, α -skeletal actin, and



α -cardiac actin) are structurally very similar, with greater than 93% identical amino acid sequences (Perrin and Ervasti, 2010). In addition, γ -actin can replace \sim 40% of α -skeletal actin in skeletal muscle sarcomeres without functional consequences (Jaeger et al., 2009). Based on these findings, we hypothesized that β -actin and γ -actin abundant in fibroblasts can be directly used for sarcomere assembly during cardiac reprogramming. We immunolabeled cells co-transduced with MGTH and LifeAct-mEmerald 4 weeks post transduction to detect cytoplasmic β - or γ -actin and sarcomeric α -actinin. We found well-organized sarcomeres exhibiting thin filaments by LifeAct expression and Z-discs by α -actinin expression (Figure 5C). However, neither β - nor γ -actin was expressed in iCMs clearly showing sarcomere formation by sarcomeric expression of LifeAct and α -actinin. Similarly, we confirmed that neither β - nor γ -actin was expressed in iCMs, which exhibited M-bands by Titin-eGFP expression and Z-discs in sarcomeres (Figure 5D). In contrast, α -cardiac actin was strongly induced and assembled into sarcomeres of iCMs detected by sarcomeric expression of LifeAct or Titin-eGFP and α -actinin (Figures 5E and 5F). These results suggest that the fibroblast actin cytoskeleton, which is largely composed of β -actin and γ -actin, is suppressed, while at the same time α -cardiac actin, which is normally absent in fibroblasts, is induced and assembled into myofibrillar contractile structures during cardiac reprogramming. The magnified views showed a precisely aligned, non-overlapping pattern between M-band and Z-disc or I-band structures (Figure 5F). Although there was a relatively small fraction of cells exhibiting both organized sarcomeres and α SMA expression (Figures 3C and 3D), we did not observe the iCMs displaying both sarcomere assembly and β - or γ -actin expression. We also analyzed expression of all six actin isoforms during cardiac reprogramming using qPCR and immunoblotting. While mRNA expressions of β -actin, γ -actin, α SMA, and γ SMA were significantly decreased, those of α -skeletal actin and α -cardiac actin were significantly increased, with the increase in α -cardiac actin being much greater than that of α -skeletal actin (Figure 5G). Of note, γ SMA and α -skeletal actin proteins were not detected by immunoblotting with or without MGTH transduction (data not shown), while α -cardiac actin, which was undetectable at baseline, was induced by cardiac reprogramming (Figure 5H). β -actin, γ -actin, and α SMA protein levels were significantly decreased by cardiac reprogramming (Figures 5H and 5I). These results suggest that significant remodeling of actin isoforms takes place during cardiac reprogramming.

Inhibition of β -actin organization in fibroblasts enhances cardiac reprogramming

Since spontaneous development of MF cytoskeletal structures counteracts induction of sarcomeres in fibroblasts

during cardiac reprogramming, we hypothesized that inhibition of actin bundling, which is required for development of MF cytoskeletal structures (Pellegrin and Mellor, 2007), enhances cardiac reprogramming. To inhibit organization of β -actin filaments, we utilized cytoplasmic β -actin fusion peptide (β -CA-FP), which contains the β -actin N-terminal amino acid sequence, and Antennapedia third helix sequence, which allows cell penetration. As previously described (Hinz et al., 2002), this peptide specifically destroys actin bundling without significant effects on α SMA expression (Figure 6A). On the day after MGTH transduction into Titin-eGFP MEFs, we exposed cells to β -CA-FP daily for 10 days. We analyzed expression of Titin-eGFP after 4 weeks (Figures 6B and 6C). Significantly more Titin-eGFP⁺ cells were observed in β -CA-FP-treated cells compared with control cells. To examine sarcomere assembly, we transduced WT MEFs with MGTH and immunostained them for α -actinin and Myomesin 4 weeks post transduction. We found there to be a much higher fraction of β -CA-FP-treated cells, with organized sarcomeres exhibiting both Z-disc and M-band structures than controls (Figures 6D and 6E). We evaluated calcium oscillation of reprogrammed cells following sequential transduction of GCaMP reporter and MGTH with or without β -CA-FP treatment. There were more GCaMP⁺ cells in β -CA-FP-treated MEF culture than in the control (Figure 6F). We also found that β -CA-FP exposure significantly increased the number of beating iCMs (Figure 6G; Videos S9 and S10). Next, we analyzed regulation of cardiac and fibroblast genes in the context of β -CA-FP treatment using qPCR. β -CA-FP treatment significantly upregulated the expression of cardiac genes, but did not significantly regulate the expression of fibroblast genes, in comparison with the control (Figure S3). Taken together, our results demonstrated that inhibition of β -actin organization enhances induction of sarcomere formation and contractility of reprogrammed cells during cardiac reprogramming.

Genetic deletion of γ -actin enhances cardiac reprogramming

Given that neither β - nor γ -actin is expressed in iCMs displaying organized sarcomeres (Figure 5), we hypothesized that deletion of either β - or γ -actin, which is a predominant cytoplasmic actin in fibroblasts, facilitates cardiac reprogramming. To test this hypothesis, we genetically knocked out γ -actin using MEFs isolated from *Actg1^{fl/fl}* mice (Sonnenmann et al., 2006). We demonstrated that γ -actin expression was markedly decreased following infection of adenovirus encoding Cre (Ad-Cre) into *Actg1^{fl/fl}* MEFs (Figures 7A and 7B). Two days after transduction of MGTH, we transduced cells with Ad-Cre or control vector (Ad-vector). Four weeks later, we immunolabeled cells to detect sarcomeric α -actinin and found that α -actinin⁺ cells

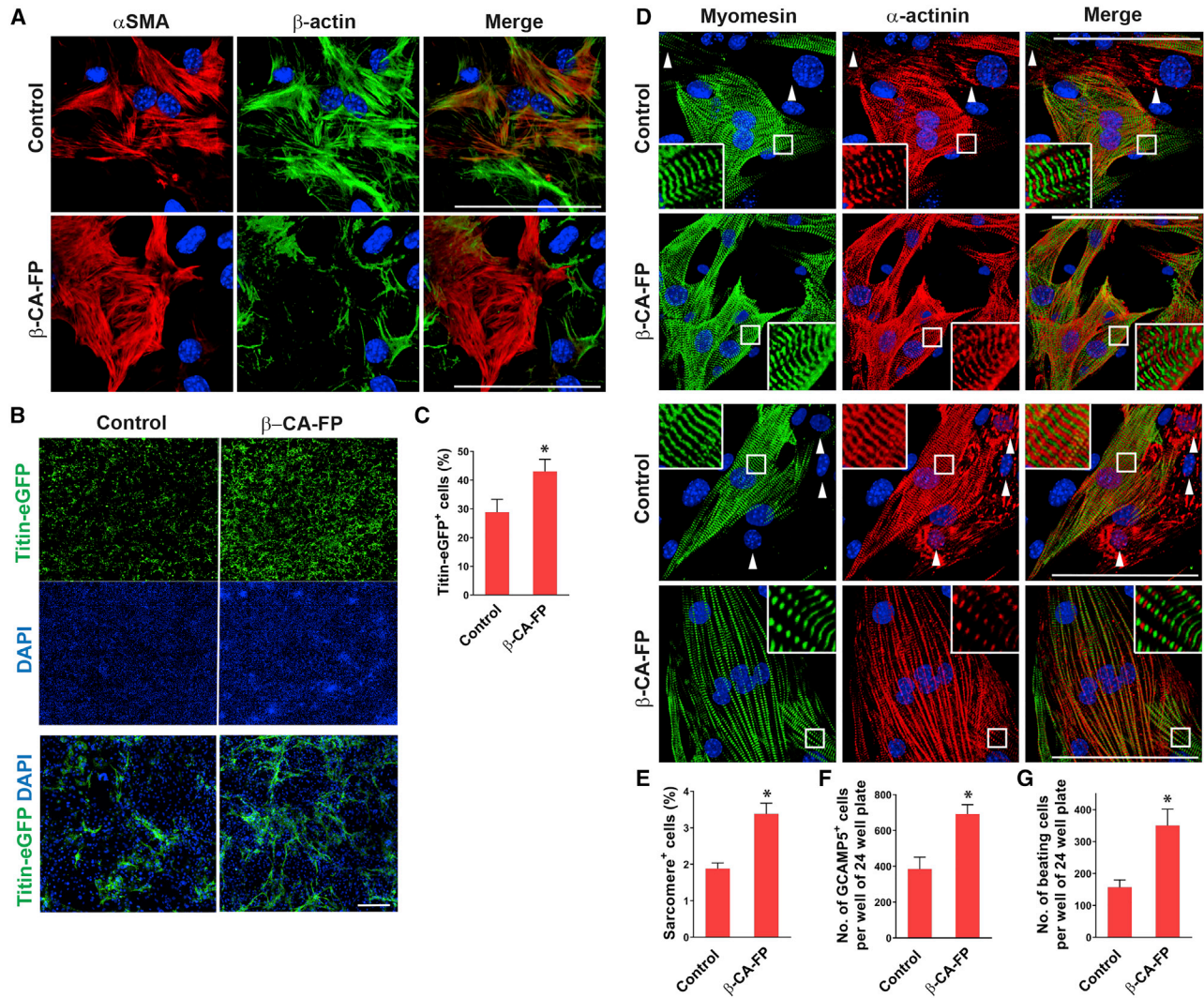


Figure 6. Inhibition of β -actin organization by β -CA-FP enhances cardiac reprogramming

(A) Inhibition of β -actin bundling by β -CA-FP treatment. One day after treating β -CA-FP or PBS (control) on WT MEFs, cells were immunostained for α SMA and β -actin.

(B and C) Inhibition of sarcomeric protein induction by β -CA-FP treatment during cardiac reprogramming. Titin-eGFP⁺ cells were quantified using high-content imaging analysis. Representative composite images (top) used for high-content imaging analysis and individual 10 \times images (bottom) are presented (B). Scale bar, 200 μ m. Seven independent experiments are presented as mean \pm SD. (C). *p < 0.05.

(D and E) Improved sarcomere assembly by β -CA-FP treatment. Enlarged views in insets show M-band (Myomesin) and Z-disc (α -actinin) structures in sarcomeres. Arrowheads indicate the cells that express α -actinin and/or Myomesin but fail to assemble sarcomeres (D). Scale bars, 100 μ m. (E) The percentage of cells exhibiting both M-bands and Z-discs among the whole population of cells was quantified. Three independent experiments are presented as mean \pm SD. *p < 0.05.

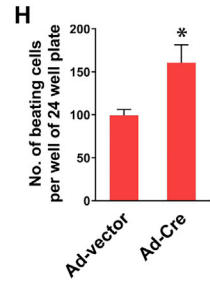
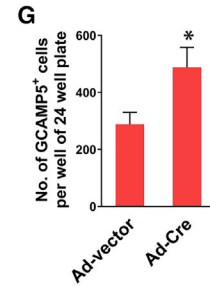
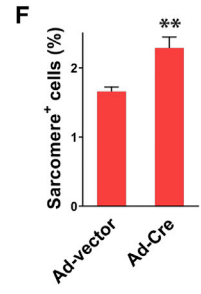
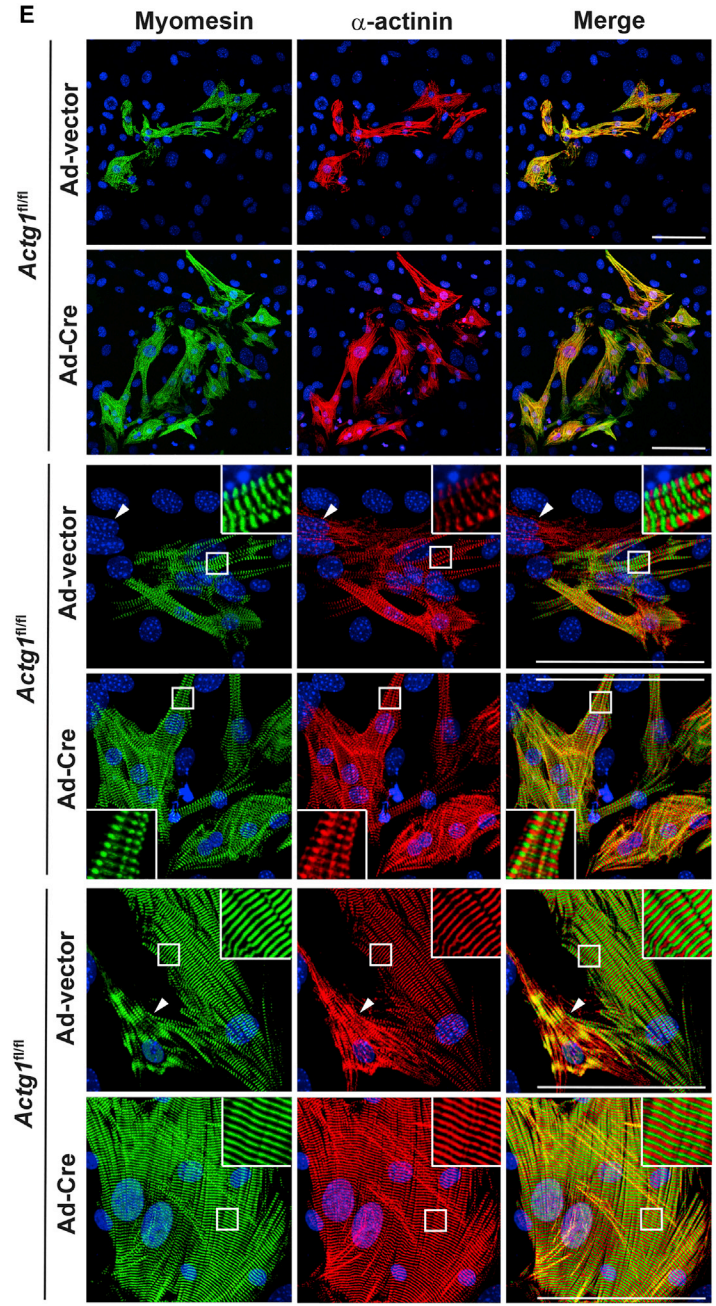
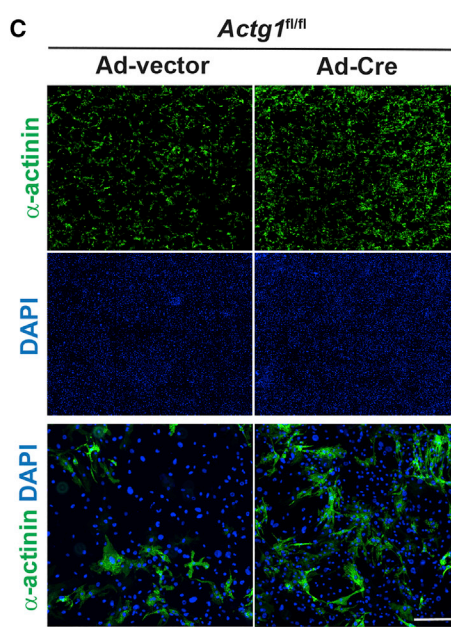
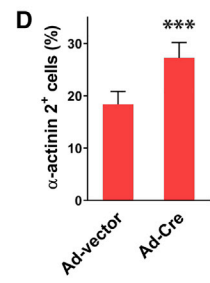
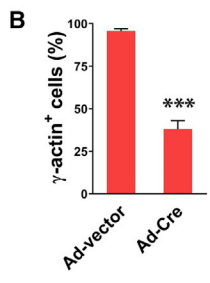
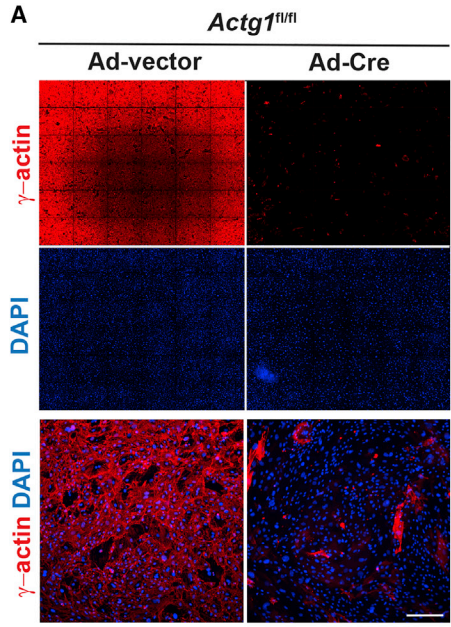
(F) Quantification of GCaMP⁺ cells following MGTH transduction with or without β -CA-FP treatment. Calcium oscillation identified by flashing green fluorescence was quantified. Four independent experiments are presented as mean \pm SD. *p < 0.05.

(G) Quantification of beating iCMs following MGTH transduction with or without β -CA-FP treatment. Four independent experiments are presented as mean \pm SD. *p < 0.05.

See also Videos S9 and S10.

(%) were significantly increased by loss of γ -actin following MGTH transduction when compared with control cells (Figures 7C and 7D). Next, we assessed sarcomere assembly in the context of genetic deletion of *Actg1* during cardiac re-

programming by immunostaining cells for α -actinin and Myomesin. A significant increase in the number of cells demonstrating both Z-disc and M-band structures was observed in Ad-Cre-infected *Actg1*^{fl/fl} MEFs compared



(legend on next page)



with Ad-vector-infected cells (Figures 7E and 7F). We quantified spontaneous oscillation of real-time GCaMP in Ad-Cre-infected cells compared with Ad-vector-infected cells. More GCaMP⁺ cells were observed in γ -actin-depleted cells than in control cells (Figure 7G). We also confirmed that the number of beating cells was increased in γ -actin-depleted MEFs (Figure 7H). In addition, to evaluate the global influence of γ -actin depletion on the reprogramming process of cardiac and fibroblast transcriptome, we performed qPCR experiments to analyze the expression of cardiac and fibroblast genes. We found significantly increased expression of cardiac genes in γ -actin-depleted cells compared with control cells (Figure S4). However, there was no significant change in expression of fibroblast genes by γ -actin depletion. Taken together, our results demonstrated that genetic deletion of a major actin component in fibroblasts can facilitate structural and functional development of iCMs, suggesting that fibroblast actin filaments function as a roadblock for cardiac reprogramming.

DISCUSSION

Fibroblast-to-iCM conversion by cardiac reprogramming has to take place in the context of ongoing fibroblast to MF differentiation *in vitro* and *in vivo*. However, how fibroblasts adopt a CM fate during their spontaneous differentiation toward MFs remains unknown. In this study, we found that most iCMs defined by their structures and contractile functions are directly reprogrammed from fibroblasts without transition through the MF state. Importantly, we demonstrated that this direct fate switch requires the remodeling of actin isoforms by which α -cardiac actin, which is normally absent in fibroblast, is induced, while α SMA, β -actin, and γ -actin, which are major components of the MF actin cytoskeleton, are significantly decreased. Our data suggest that cardiac reprogramming has to

compete with the fibroblast differentiation process to build sarcomeres in the same cytoplasm, which otherwise becomes filled with organized stress fibers.

To establish a new cell fate in fibroblasts, the reprogramming process has to intervene in the fibroblast differentiation process, which simultaneously progresses *in vitro* and *in vivo* in response to mechanical stress. Fibroblast differentiation requires the organization of actin filaments involving β -actin, γ -actin, and α SMA to generate isometric contractile force. The resulting MF cytoskeleton, referred to as stress fiber, is a primitive form of contractile unit only capable of isometric contraction, while the sarcomere is considered as a professional form of contractile unit for isotonic contraction. Stress fiber formation and MF differentiation are readily recapitulated by culturing fibroblasts in a plastic dish owing to high isometric tension created by the stiff surface of a culture dish *in vitro*. Thus, during cardiac reprogramming *in vitro* and *in vivo*, cardiac contractile structures should be built upon a fibroblast cytoskeleton, which spontaneously becomes organized in response to injury or in culture. From a structural point of view, cardiac reprogramming may be defined as the intracellular process that replaces “primitive” isometric contractile structures with “professional” isotonic contractile structures in the fibroblast cytoplasm.

Myofibril assembly in striated muscle during development is a highly conserved process from jellyfish to human (Seipel and Schmid, 2005). Although how myofibril is assembled is not entirely clear, multiple studies have suggested that myofibril is formed from the premyofibril structure, which resembles the structure of stress fiber composed of actin filaments, α -actinin, and non-muscle myosin (Sanger et al., 2005). Thus, we suspected that the stress fiber structure may serve as a template of cardiac reprogramming by providing β - or γ -actin as a building block for sarcomere assembly, analogous to the proposed premyofibril model for myofibrillogenesis during striated muscle development.

Figure 7. Loss of γ -actin enhances cardiac reprogramming

(A and B) Decrease of γ -actin expression by Ad-Cre infection into *Actg1*^{fl/fl} MEFs. One week after Ad-Cre or Ad-vector infection into *Actg1*^{fl/fl} MEFs, cells were immunostained for γ -actin. Representative composite images (top) used for high-content imaging analysis and individual 10 \times images (bottom) are presented (A). Scale bar, 200 μ m. Quantification of γ -actin⁺ cells is summarized (B). Three independent experiments are presented as mean \pm SD. ****p* < 0.0005.

(C and D) Increased sarcomeric protein induction by loss of γ -actin during cardiac reprogramming. Representative composite images (top) used for high-content imaging analysis and individual 10 \times images (bottom) are presented (C). Scale bar, 200 μ m. Quantification of α -actinin⁺ cells is summarized (D). Six independent experiments are presented as mean \pm SD. **p* < 0.05.

(E and F) Enhanced sarcomere assembly by loss of γ -actin during cardiac reprogramming. Enlarged views in insets show M-band structures (Myomesin) and Z-disc structures (α -actinin) in sarcomeres. Arrowheads indicate the cells that express α -actinin and/or Myomesin but fail to fully assemble sarcomeres. Scale bars, 100 μ m. The percentage of cells exhibiting both M-bands and Z-discs was quantified (F). Five independent experiments are presented as mean \pm SD. ***p* < 0.01.

(G) Quantification of GCaMP⁺ cells following sequential transduction of TroponinT-GCaMP5-Zeo reporter construct, MGTH, and Ad-Cre or Ad-vector. Calcium oscillation identified by flashing green fluorescence was quantified. Four independent experiments are presented as mean \pm SD. **p* < 0.05.

(H) Quantification of beating iCMs. Three independent experiments are presented as mean \pm SD. **p* < 0.05.



However, our results showed the opposite. Pre-existing β - and γ -actins were markedly decreased during cardiac reprogramming while α -cardiac actin, which is normally absent in fibroblasts, was directly induced and assembled into sarcomeres. Furthermore, assembly of non-cardiac actin filaments inhibits sarcomere formation during cardiac reprogramming. Pharmacological or genetic disruption of β - or γ -actin does not inhibit but improves structural and functional development of iCMs. Taken together, our study demonstrated that pre-existing fibroblast actin filaments serve as a structural hurdle for cardiac reprogramming instead of a template for iCM generation, suggesting a distinct model for myofibrillogenesis during cardiac reprogramming.

An iCM has been implicitly defined as a cell inducing sarcomeric proteins following cardiac reprogramming. However, sarcomeric protein induction alone does not reflect the success of cardiac reprogramming. Although necessary, it is far from sufficient to define an iCM. In fact, a major fraction of sarcomeric protein-expressing cells following cardiac reprogramming fails to develop the sarcomere, which is a defining feature of striated muscle cells such as CMs (Nam et al., 2014). Our study provided a mechanistic insight into why structural development of iCMs is so inefficient following cardiac reprogramming. We showed that the simultaneous development of MF structures in fibroblasts counteracts sarcomere development in the same cytoplasm. A majority of cells fail to fully commit to a CM fate, probably because of simultaneous progression of mutually exclusive, two-cell fate paths in fibroblasts during cardiac reprogramming. As a result, a significant fraction of cells are hybrid or have undetermined fates of cells (neither MFs nor iCMs) following cardiac reprogramming. Some of those cells have often been considered as iCMs as long as they express a sarcomeric protein. While directed pluripotent stem cell (PSC) differentiation to CMs does not go through any pre-existing structural barrier, cardiac reprogramming has to overcome pre-existing or simultaneously developing cytoskeletal structures in order to build myofibrillar structures on the fibroblast cytoplasm. This may explain, at least in part, markedly lower efficiency of inducing structured iCMs by cardiac reprogramming than by directed cardiac differentiation of PSCs.

While it was previously shown that inhibition of TGF- β signaling enhances cardiac reprogramming, we focused on how a fibroblast adopts a CM fate in the context of constant stimulation of TGF- β signaling, which leads to simultaneous fibroblast differentiation during cardiac reprogramming. Fibroblast differentiation requires organization of actin filaments consisting of β -actin, γ -actin, and α SMA. In contrast, to induce sarcomere formation in fibroblasts, cardiac reprogramming induces α -cardiac actin, which is absent in fibroblasts, while at the same time

inhibiting fibroblast actin organization. This remodeling process of actin isoforms is necessary for converting fibroblasts to structurally and functionally mature iCMs. Importantly, our study shows that simply inducing sarcomeric proteins without completing structural remodeling processes fails to generate bona fide iCMs. Inadvertently, our results revealed that suppression of MF activation may be not the major mechanism by which TGF- β inhibition increases iCM generation, pointing to the presence of other mechanisms. In this regard, a recent study showed that suppression of canonical TGF- β signaling promotes cardiac reprogramming by enhancing interaction of Gata4 with H3K27me3 demethylase JMJD3 (Riching et al., 2021).

EXPERIMENTAL PROCEDURES

Mice

All animal procedures were performed with the approval of Vanderbilt University Medical Center. Titin-eGFP reporter knockin mice were a gift of Dr. Gotthardt (da Silva Lopes et al., 2011). α SMA^{Cre} mice were a gift of Dr. Kalluri (LeBleu et al., 2013). α SMA^{-/-} mice were generated by intercrossing α SMA^{+/-} mice obtained from Dr. Schwartz (Schildmeyer et al., 2000). Generation of *Actg1*^{fl/fl} mice was described previously (Sonnemann et al., 2006).

In vitro cardiac reprogramming

pBabe-X retroviral constructs were transfected into Platinum E cells (Cell Biolabs) using Fugene 6 (Promega). Platinum E cells were replenished with the fresh growth medium (Dulbecco's modified Eagle's medium [DMEM] with 10% fetal bovine serum [FBS] and 1% penicillin/streptomycin) 16–20 h after transfection. A flat-bottomed 24 well plate (Ibidi) was coated with human fibronectin (Sigma, F2006) for 24 h at 37°C. MEFs were plated into a fibronectin-coated 24-well plate about 24 h before infection. The viral medium was collected and filtered through a 0.45- μ m polyethersulfone filter at 48 h post transfection. The fibroblast growth medium in the cell-culture plate was replaced with the viral medium supplemented with Polybrene at a concentration of 6 μ g/mL. Twenty-four hours after infection, the viral medium was replaced with the cardiac induction medium composed of DMEM/199 (4:1), 10% FBS, 5% horse serum, 1% penicillin/streptomycin, 1% non-essential amino acids, 1% essential amino acids, 1% B-27, 1% insulin-selenium-transferrin, 1% vitamin mixture, and 1% sodium pyruvate (Invitrogen), 1 μ M SB431542 (Sigma, S4317), and 0.5 μ M A83-01 (Tocris, 2939). The induction medium was changed every 3 days until cells were fixed. β -CA-FP (acetyl Asp-Asp-Asp-Ile-Ala-Arg-Gln-Ile-Lys-Ile-Trp-Phe-Pro-Asn-Arg-Arg-Met-Lys-Trp-Lys-Lys-NH₂) was generated by Biomatik. β -CA-FP (50 μ g/mL) resolved in the cardiac induction medium was replaced daily for 10 days after transduction.

SUPPLEMENTAL INFORMATION

Supplemental information can be found online at <https://doi.org/10.1016/j.stemcr.2022.05.004>.



AUTHOR CONTRIBUTIONS

Conceptualization, Y.-J.N.; methodology, Z.Z., L.J.S., Z.S., J.M.E., and Y.-J.N.; formal analysis, Z.Z. and R.B.; investigation, Z.Z., W.Z., R.B., and Y.-J.N.; resources, Z.Z., L.J.S., Z.S., D.C.R., and J.M.E.; data curation, Z.Z. and Y.-J.N.; writing – original draft, Z.Z. and Y.-J.N.; writing – review and editing, all authors; supervision, D.C.R., J.M.E., and Y.-J.N.; funding acquisition, Z.Z., J.M.E., and Y.-J.N.

ACKNOWLEDGMENTS

High-content imaging analysis was performed in the Vanderbilt High-Throughput Screening (HTS) Core Facility. The HTS Core receives support from the Vanderbilt Institute of Chemical Biology and the Vanderbilt-Ingram Cancer Center (P30 CA68485). We appreciate the technical assistance by Dr. Boris Hinz. We thank Dr. Russell Addis for the TroponinT-GCaMP5-Zeo reporter construct. This work was supported by Gilead Sciences Research Scholars Program and NIH (R01 HL146524) to Y.-J.N., NIH (R01 AR049899) to J.M.E., and AHA (20POST35210170) to Z.Z.

CONFLICTS OF INTEREST

The authors declare no competing interests.

Received: January 18, 2022

Revised: May 12, 2022

Accepted: May 13, 2022

Published: June 9, 2022

REFERENCES

Addis, R.C., Ifkovits, J.L., Pinto, F., Kellam, L.D., Estes, P., Rentschler, S., Christoforou, N., Epstein, J.A., and Gearhart, J.D. (2013). Optimization of direct fibroblast reprogramming to cardiomyocytes using calcium activity as a functional measure of success. *J. Mol. Cell. Cardiol.* *60*, 97–106. <https://doi.org/10.1016/j.jmcc.2013.04.004>.

Bektik, E., Dennis, A., Pawlowski, G., Zhou, C., Maleski, D., Takahashi, S., Laurita, K.R., Deschenes, I., and Fu, J.D. (2018). S-phase synchronization facilitates the early progression of induced-cardiomyocyte reprogramming through enhanced cell-cycle exit. *Int. J. Mol. Sci.* *19*, 1364. <https://doi.org/10.3390/ijms19051364>.

Benjamin, E.J., Virani, S.S., Callaway, C.W., Chamberlain, A.M., Chang, A.R., Cheng, S., Chiuve, S.E., Cushman, M., Delling, F.N., Deo, R., et al. (2018). Heart disease and stroke statistics-2018 update A report from the American heart association. *Circulation* *137*, E67–E492. <https://doi.org/10.1161/CIR.0000000000000558>.

Clark, K.A., McElhinny, A.S., Beckerle, M.C., and Gregorio, C.C. (2002). Striated muscle cytoarchitecture: an intricate web of form and function. *Annu. Rev. Cell Dev. Biol.* *18*, 637–706. <https://doi.org/10.1146/annurev.cellbio.18.012502.105840>.

da Silva Lopes, K., Pietas, A., Radke, M.H., and Gotthardt, M. (2011). Titin visualization in real time reveals an unexpected level of mobility within and between sarcomeres. *J. Cell Biol.* *193*, 785–798. <https://doi.org/10.1083/jcb.201010099>.

Darby, I., Skalli, O., and Gabbiani, G. (1990). Alpha-smooth muscle actin is transiently expressed by myofibroblasts during experimental wound healing. *Lab. Invest.* *63*, 21–29.

Fu, Y., Huang, C., Xu, X., Gu, H., Ye, Y., Jiang, C., Qiu, Z., and Xie, X. (2015). Direct reprogramming of mouse fibroblasts into cardiomyocytes with chemical cocktails. *Cell Res.* *25*, 1013–1024. <https://doi.org/10.1038/cr.2015.99>.

Gautel, M. (2011). The sarcomeric cytoskeleton: who picks up the strain? *Curr. Opin. Cell Biol.* *23*, 39–46. <https://doi.org/10.1016/j.ceb.2010.12.001>.

Hinz, B. (2010). The myofibroblast: paradigm for a mechanically active cell. *J. Biomech.* *43*, 146–155. <https://doi.org/10.1016/j.jbiomech.2009.09.020>.

Hinz, B., Celetta, G., Tomasek, J.J., Gabbiani, G., and Chaponnier, C. (2001). Alpha-smooth muscle actin expression upregulates fibroblast contractile activity. *Mol. Biol. Cell* *12*, 2730–2741. <https://doi.org/10.1091/mbc.12.9.2730>.

Hinz, B., Gabbiani, G., and Chaponnier, C. (2002). The NH₂-terminal peptide of alpha-smooth muscle actin inhibits force generation by the myofibroblast in vitro and in vivo. *J. Cell Biol.* *157*, 657–663. <https://doi.org/10.1083/jcb.200201049>.

Hotulainen, P., and Lappalainen, P. (2006). Stress fibers are generated by two distinct actin assembly mechanisms in motile cells. *J. Cell Biol.* *173*, 383–394. <https://doi.org/10.1083/jcb.200511093>.

Humeres, C., and Frangogiannis, N.G. (2019). Fibroblasts in the infarcted, remodeling, and failing heart. *JACC Basic Transl. Sci.* *4*, 449–467. <https://doi.org/10.1016/j.jacbts.2019.02.006>.

Ieda, M., Fu, J.D., Delgado-Olguin, P., Vedantham, V., Hayashi, Y., Bruneau, B.G., and Srivastava, D. (2010). Direct reprogramming of fibroblasts into functional cardiomyocytes by defined factors. *Cell* *142*, 375–386. <https://doi.org/10.1016/j.cell.2010.07.002>.

Ifkovits, J.L., Addis, R.C., Epstein, J.A., and Gearhart, J.D. (2014). Inhibition of TGF β signaling increases direct conversion of fibroblasts to induced cardiomyocytes. *PLoS One* *9*, e89678. <https://doi.org/10.1371/journal.pone.0089678>.

Inagawa, K., Miyamoto, K., Yamakawa, H., Muraoka, N., Sadahiro, T., Umei, T., Wada, R., Fukuda, K., Katsumata, Y., Ieda, M., et al. (2012). Induction of cardiomyocyte-like cells in infarct hearts by gene transfer of Gata4, Mef2c, and Tbx5. *Circ. Res.* *18*, S146–S1156. <https://doi.org/10.1016/j.cardfail.2012.08.114>.

Jaeger, M.A., Sonnemann, K.J., Fitzsimons, D.P., Prins, K.W., and Ervasti, J.M. (2009). Context-dependent functional substitution of alpha-skeletal actin by gamma-cytoplasmic actin. *FASEB J.* *23*, 2205–2214. official publication of the Federation of American Societies for Experimental Biology. <https://doi.org/10.1096/fj.09-129783>.

Jayawardena, T.M., Egemnazarov, B., Finch, E.A., Zhang, L., Payne, J.A., Pandya, K., Zhang, Z., Rosenberg, P., Mirosou, M., and Dzau, V.J. (2012). MicroRNA-mediated in vitro and in vivo direct reprogramming of cardiac fibroblasts to cardiomyocytes. *Circ. Res.* *110*, 1465–1473. <https://doi.org/10.1161/circresaha.112.269035>.

Kurotsu, S., Sadahiro, T., Fujita, R., Tani, H., Yamakawa, H., Tamura, F., Isomi, M., Kojima, H., Yamada, Y., Abe, Y., et al. (2020). Soft matrix promotes cardiac reprogramming via inhibition of YAP/TAZ and suppression of fibroblast signatures. *Stem Cell Rep.* *15*, 612–628. <https://doi.org/10.1016/j.stemcr.2020.07.022>.



- Leask, A. (2007). TGF β , cardiac fibroblasts, and the fibrotic response. *Cardiovasc. Res.* 74, 207–212. <https://doi.org/10.1016/j.cardiores.2006.07.012>.
- LeBleu, V.S., Taduri, G., O'Connell, J., Teng, Y., Cooke, V.G., Woda, C., Sugimoto, H., and Kalluri, R. (2013). Origin and function of myofibroblasts in kidney fibrosis. *Nat. Med.* 19, 1047–1053. <https://doi.org/10.1038/nm.3218>.
- Mohamed, T.M., Stone, N.R., Berry, E.C., Radzinsky, E., Huang, Y., Pratt, K., Ang, Y.S., Yu, P., Wang, H., Tang, S., et al. (2016). Chemical enhancement of in vitro and in vivo direct cardiac reprogramming. *Circulation* 135, 978–995.
- Nam, Y.J., Lubczyk, C., Bhakta, M., Zang, T., Fernandez-Perez, A., McAnally, J., Bassel-Duby, R., Olson, E.N., and Munshi, N.V. (2014). Induction of diverse cardiac cell types by reprogramming fibroblasts with cardiac transcription factors. *Development* 141, 4267–4278. <https://doi.org/10.1242/dev.114025>.
- Pellegrin, S., and Mellor, H. (2007). Actin stress fibres. *J. Cell Sci.* 120, 3491–3499. <https://doi.org/10.1242/jcs.018473>.
- Perrin, B.J., and Ervasti, J.M. (2010). The actin gene family: function follows isoform. *Cytoskeleton (Hoboken)* 67, 630–634. <https://doi.org/10.1002/cm.20475>.
- Qian, L., Huang, Y., Spencer, C.I., Foley, A., Vedantham, V., Liu, L., Conway, S.J., Fu, J.D., and Srivastava, D. (2012). In vivo reprogramming of murine cardiac fibroblasts into induced cardiomyocytes. *Nature* 485, 593–598. <https://doi.org/10.1038/nature11044>.
- Riching, A.S., Danis, E., Zhao, Y., Cao, Y., Chi, C., Bagchi, R.A., Klein, B.J., Xu, H., Kutateladze, T.G., McKinsey, T.A., et al. (2021). Suppression of canonical TGF-beta signaling enables GATA4 to interact with H3K27me3 demethylase JMJD3 to promote cardiomyogenesis. *J. Mol. Cell. Cardiol.* 153, 44–59. <https://doi.org/10.1016/j.yjmcc.2020.12.005>.
- Riedl, J., Crevenna, A.H., Kessenbrock, K., Yu, J.H., Neukirchen, D., Bista, M., Bradke, F., Jenne, D., Holak, T.A., Werb, Z., et al. (2008). Lifeact: a versatile marker to visualize F-actin. *Nat. Methods* 5, 605–607. <https://doi.org/10.1038/nmeth.1220>.
- Sandbo, N., and Dulin, N. (2011). Actin cytoskeleton in myofibroblast differentiation: ultrastructure defining form and driving function. *Transl. Res.* 158, 181–196. <https://doi.org/10.1016/j.trsl.2011.05.004>.
- Sanger, J.W., Kang, S., Siebrands, C.C., Freeman, N., Du, A., Wang, J., Stout, A.L., and Sanger, J.M. (2005). How to build a myofibril. *J. Muscle Res. Cell Motil.* 26, 343–354. <https://doi.org/10.1007/s10974-005-9016-7>.
- Schildmeyer, L.A., Braun, R., Taffet, G., Debiase, M., Burns, A.E., Bradley, A., and Schwartz, R.J. (2000). Impaired vascular contractility and blood pressure homeostasis in the smooth muscle alpha-actin null mouse. *FASEB J.* 14, 2213–2220. official publication of the Federation of American Societies for Experimental Biology. <https://doi.org/10.1096/fj.99-0927.com>.
- Seipel, K., and Schmid, V. (2005). Evolution of striated muscle: jellyfish and the origin of triploblasty. *Dev. Biol.* 282, 14–26. <https://doi.org/10.1016/j.ydbio.2005.03.032>.
- Song, K., Nam, Y.J., Luo, X., Qi, X., Tan, W., Huang, G.N., Acharya, A., Smith, C.L., Tallquist, M.D., Neilson, E.G., et al. (2012). Heart repair by reprogramming non-myocytes with cardiac transcription factors. *Nature* 485, 599–604. <https://doi.org/10.1038/nature11139>.
- Sonnemann, K.J., Fitzsimons, D.P., Patel, J.R., Liu, Y., Schneider, M.F., Moss, R.L., and Ervasti, J.M. (2006). Cytoplasmic gamma-actin is not required for skeletal muscle development but its absence leads to a progressive myopathy. *Dev. Cell* 11, 387–397. <https://doi.org/10.1016/j.devcel.2006.07.001>.
- Tomasek, J.J., Gabbiani, G., Hinz, B., Chaponnier, C., and Brown, R.A. (2002). Myofibroblasts and mechano-regulation of connective tissue remodelling. *Nat. Rev. Mol. Cell Biol.* 3, 349–363. <https://doi.org/10.1038/nrm809>.
- Tschumperlin, D.J., Ligresti, G., Hilscher, M.B., and Shah, V.H. (2018). Mechanosensing and fibrosis. *J. Clin. Invest.* 128, 74–84. <https://doi.org/10.1172/jci93561>.
- Umei, T.C., Yamakawa, H., Muraoka, N., Sadahiro, T., Isomi, M., Haginiwa, S., Kojima, H., Kurotsu, S., Tamura, F., Osakabe, R., et al. (2017). Single-construct polycistronic doxycycline-inducible vectors improve direct cardiac reprogramming and can be used to identify the critical timing of transgene expression. *Int. J. Mol. Sci.* 18, 1805. <https://doi.org/10.3390/ijms18081805>.
- van Putten, S., Shafieyan, Y., and Hinz, B. (2016). Mechanical control of cardiac myofibroblasts. *J. Mol. Cell. Cardiol.* 93, 133–142. <https://doi.org/10.1016/j.yjmcc.2015.11.025>.
- Zhang, Z., Zhang, A.D., Kim, L.J., and Nam, Y.J. (2019a). Ensuring expression of four core cardiogenic transcription factors enhances cardiac reprogramming. *Sci. Rep.* 9, 6362. <https://doi.org/10.1038/s41598-019-42945-w>.
- Zhang, Z., Zhang, W., and Nam, Y.J. (2019b). Stoichiometric optimization of Gata4, Hand2, Mef2c, and Tbx5 expression for contractile cardiomyocyte reprogramming. *Sci. Rep.* 9, 14970. <https://doi.org/10.1038/s41598-019-51536-8>.
- Zhao, Y., Londono, P., Cao, Y., Sharpe, E.J., Proenza, C., O'Rourke, R., Jones, K.L., Jeong, M.Y., Walker, L.A., Buttrick, P.M., et al. (2015). High-efficiency reprogramming of fibroblasts into cardiomyocytes requires suppression of pro-fibrotic signalling. *Nat. Commun.* 6, 8243. <https://doi.org/10.1038/ncomms9243>.